Mechanisms of microparticle propulsion by laser ablation

A. B. Gojani[1], V. Menezes[2], J. J. Yoh[1], K. Takayama[3]

[1] Mechanical and Aerospace Department, Seoul National University, Republic of Korea,
[2] Department of Aerospace Engineering, Indian Institute of Technology, Bombay, Mumbai 400 076, India,
[3] Interdisciplinary Shock Wave Center, TUBERO, Tohoku University, Sendai, Japan

Keywords: Microparticle, shock wave, laser ablation, medical application.

Abstract

Propulsion of gene coated micro-particles is desired for non-intrusive drug delivery inside biological tissue. This has been achieved by the development of a device that uses high power laser pulses. The present paper looks at the mechanisms of micro-particle acceleration. Initially, a high power laser pulse is focused onto the front side of a thin aluminium foil leading to its ablation. The ablation front drives a compression wave inside the foil, thus leading to the formation of a shock wave, which will later reflect from the rear side of the foil, due to acoustic impedance mismatch. The reflected wave will induce an opposite motion of the foil, characterized by a very high speed, of the order of several millimeters per microsecond. Micro-particles, which are deposited on the rear side of the foil, thus get accelerated and ejected as micro-projectiles and are able to penetrate several hundreds of micrometers inside tissue-like material. These processes have been observed experimentally by using high-speed shadowgraphy and considered analytically.

Introduction

Propulsion phenomena and challenges are usually connected to setting a massive body, such as a rocket, into motion by means of chemical transfer of energy, so that it can reach distant places. This paper tries to present a different application of propulsion: we are concerned with setting micro-bodies into motion so that they can reach places beneath our skin. The research in this field is motivated by the need to deliver gene coated microparticles into living tissue for purposes of genetic engineering or vaccination. This problem has been attacked by means of particle gun based device [1)], or by using pressurized helium in a shock tube based system [2)]. An alternative approach to microparticle acceleration is by utilizing impulse transfer from laser ablation of a metal foil to a microlayer of particles resting on the rear side of the foil [3)]. This technique has several advantages over the above mentioned devices: it can be combined with optical fibers, thus the drug holding part can be miniaturized to millimeter levels, as well as deliver drugs to internal organs in a very localized area, if attached to an endoscope-like fiber; it also eliminates risks associated with syringe vaccination, such as infections; it is non-intrusive and painless. Laser ablation has been considered for propulsion of the ablated material [4)]. Ablative laser propulsion would produce thrust by heating a propellant to high enough temperatures, such that vapor or plasma jet would result from the ablated material, thus inducing thrust.

Theory

The following section explains the physics behind laser ablation, shock wave generation and propagation in solids, as well as shock wave release at the end of the solid. Finally, it explains the acceleration and motion of the particles from a rapid plastic deformation of the shock loaded foil and their penetration into soft tissue. Schematic of the laser ablation and particle propulsion is shown in Fig 1.

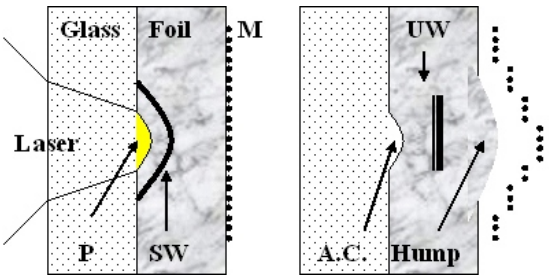

Fig 1. The schematic of the physical process of ablation (left) and particle propulsion (right). Laser irradiates from the left. P is the plasma, SW is the shock wave, M shows the microparticles, A.C. is the ablated crater, and UW is the unloaded wave. The direction of motion of the shock wave is towards the right, and for the unloaded wave is towards the left.

In general, by laser ablation is understood the process of removal of material from a condensed target due to irradiation by a short high energy laser light. When high energy density impinges on the metal foil, it is absorbed by the free electrons, which reach very high temperatures in timescales much shorter than the laser pulse duration. The absorption layer is only several nanometers thick (a few mean free paths for the electrons), but through various interactions, including multiphoton and avalanche ionization, plasma formation, plasma heating, and electron-electron relaxation and electron-phonon coupling [5)], it will expand rapidly into the surrounding ambient. For a nanosecond pulse, the expansion will start and continue even during the duration of the

pulse. The expansion of the plasma is towards the laser beam. On the other hand, part of the absorbed laser energy and deposited into the kinetic (thermal) energy of the electrons will initiate an electron thermal wave inside the target, defining an ablation front. The energy transfer from electrons to the lattice occurs in longer timescales due to the large difference in electron and ion masses. While the ablated material is moving away from the foil, the ablation front proceeds with high speeds toward the rear side of it. This will cause compression of the solid target, which ultimately generates a shock wave.

In considering these interactions of light and matter, attention should be paid to the effectiveness of coupling of the wavelength and shock wave. Metallic foils are good at reflecting visible and infrared and readily absorb ultraviolet light, which leads to the conclusion that shock wave generation can be enhanced by using shorter wavelength laser beams. But, this also leads to the lowering of the dielectric breakdown threshold, which results into lower plasma pressure peaks. A study from Berthe [6] shows that at irradiances lower than 6 GW/cm^2, 355 nm light can produce plasma pressures a few GPa higher than 1064 nm laser beam. But, pressures achieved by this short wavelength will soon saturate, while the infrared beam will continue achieving higher pressures when irradiance is increased to 10 GW/cm^2, reaching almost double the values for plasma pressures.

A simple estimate of pressure obtained by laser ablation can be described by the equation [7]

$$P_{abl} \approx 40\left(I/\lambda\right)^{2/3} \tag{1}$$

where the ablation pressure P_{abl} is expressed in Mbar (100 GPa), I is the power of the incident laser flux (irradiance), expressed in W/cm^2, and λ is the laser light wavelength. A simple estimate shows that pressures of several hundreds of kilobars up to tens of megabars can be easily achieved with laser energies of less than 1 J, if the beam is focused to a spot with diameter comparable to the diffraction limit. Placement of an overlay transparent glass confines the ablation and enables the use of lower laser energies and large focal spots [8], enhancing the shock pressures.

Once generated, the shock wave propagates through the foil as longitudinal compression wave, and its velocity in a thin metal foil can be given by

$$C_l = \sqrt{\frac{E\left(1-\nu\right)}{\rho_{foil}\left(1+\nu\right)\left(1-2\nu\right)}} \tag{2}$$

where E is the Young's modulus, ρ_{foil} is the density, and v is the Poisson's ratio of the foil.

When the shock wave reaches the rear end of the foil, it emerges from the free surface and the material unloads to atmospheric pressure. This causes a rarefaction wave to travel backward into material with the speed equal to that of sound for the state of the shocked material, and the material itself will move in the direction of the transmitted shock. This motion will result in the plastic deformation of the foil and ejection of the particles.

Motion of particles can be analyzed by dividing it into three stages. The initial stage is the acceleration of the particles due to shock wave unloading from the rear side of the ablated foil, followed by an initially hypersonic motion through air, and finally penetration into tissue, characterized by large deceleration. The time of the acceleration of the particles is rapid in comparison with the subsequent motion, hence it can be neglected and particles are considered to move with the same outlet velocity as the velocity of the displacement of the foil due to plastic deformation from shock wave unloading. This velocity can be calculated as in the following. The pressure in the foil P is related to the displacement of the foil due to plastic deformation S, by the relation

$$P = \frac{SE}{2C_l\tau} \tag{3}$$

where τ is the time it takes the shock wave to traverse the thin foil. From here, the velocity of the rear side of the foil can be calculated by the equation

$$V = \frac{PC_l}{E} \tag{4}$$

The equation of motion for particles from their propulsion till their impact on the targeted tissue is governed by the drag force

$$m\frac{dV}{dt} = -\frac{1}{2}C_d\rho_{air}V^2A \tag{5}$$

where C_d is the drag coefficient, ρ_{air} is the air density, and A is the projected area of the sphere on the target. In deriving this equation, we assume the particles are spheres and neglected their weight. After elapsing the stand-off distance S_d, the distance between the foil and the tissue, particles will reach the final velocity

$$V_i = \sqrt{V^2 - 2S_d\frac{dV}{dt}} \tag{6}$$

which is the impact velocity into the targeted tissue.

When particles penetrate the tissue, they run into large resistance, and ultimately their motion is terminated inside it. The depth of penetration can be calculated using the unified penetration model [8]. Based on this model, the force that the targeted tissue exerts on the motion of the particles is the sum of the inertial force of the targeted tissue, which accelerates from rest to the speed of the penetrating particle, and

the force needed to yield the targeted tissue, characterized by its hardness, resulting into the following equation

$$d = \frac{4\rho_{particle} r_{particle}}{3\rho_{tissue}} \left(\ln \frac{\frac{\rho_{tissue} V_i^2}{2} + 3\sigma_{tissue}}{3\sigma_{tissue}} \right) \quad (7)$$

Here, $\rho_{particle}$ and ρ_{tissue} are the densities of the particles and the tissue, $r_{particle}$ is the radius of the particle, V_i is the particle impact velocity, and σ_{tissue} is the yield strength of the tissue.

Experiment

In the following, we will give an experimental example of the ideas developed on the preceding section. This experiment was carried out at the Interdisciplinary Shock Wave Center of the Tohoku University, Sendai, Japan, with the aim of propelling microparticles for drug delivery.

The experimental setup is shown in Fig 2. It consists of the ablation laser, the directing optics, focusing optics, foil/particle holder, and soft target as a model of the tissue. The shadowgraph setup for visualization is not shown.

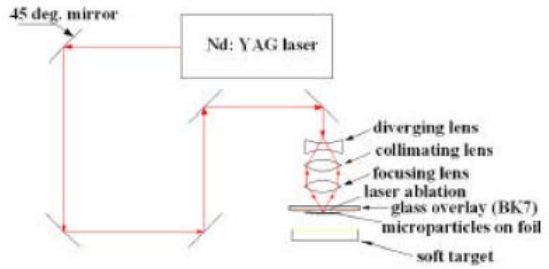

Fig. 2. The experimental setup for particle propulsion using laser ablation.

The ablation of the foil was achieved by a Q-switched Nd:YAG laser, emitting 1064 nm wavelength light with pulse duration of 5 ns and energy of 1.4 J/pulse.

The laser beam was directed by mirrors to a system of diverging and converging lenses. The 9 mm beam that exits the laser was expanded and then collimated by a concave and convex lens, and then finally focused using a short focal length convex lens into a focal spot, with a typical diameter of the order of a millimeter. This beam, before reaching the target for ablation, will pass through a 3-5 mm thick overlaid BK7 glass, which is used to confine the ablation.

The ablated foil was pure aluminum with 100 um thickness. Particles that were accelerated in this experiment were 1 μm diameter tungsten particles. They were initially submerged in alcohol (C2H5OH or 2-propanol) and then a small volume of this mixture, usually 2.5 - 10 μ*l*, is deposited on the thin foil. The alcohol will evaporate in a matter of seconds, leaving a thin trace of particles, as shown in Fig. 3. The distribution and density of particles can be adjusted by changing the concentration of particles in the mixture. In these experiments tungsten particles were chosen since they have similar density to gold, thus making the experiments cost effective. In real life applications, one would want to use gold particles, because small quantities of gold do not harm human tissue, due to its biological inertness [10].

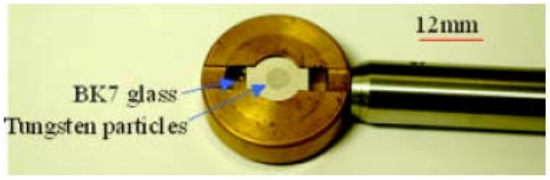

Fig. 3. Foil/particle holder with a thin layer of 1 μm tungsten particles deposited on a thin aluminum foil.

Diagnostics used for these experiments was a shadowgraph system equipped with a high-speed video camera (Shimadzu HPV-1). This camera is capable of recording 100 frames with a maximum speed of 1 Megaframes per second. Light source for shadowgraph was provided by a continuous 5 mW HeNe laser.

In two set of experiments, particles were delivered into a soft target made of 3% gelatin weight ratio to water, and into the liver tissue of an experimental rat. Gelatin mixture was prepared by completely dissolving gelatin into water at 60 °C, and then cooling it to room temperatures, so that a soft pasty mass would result. This matter represent human thrombus model.

A series of shadowgraph images of the microparticles being propelled by laser ablation is shown in Fig. 4. From these images we can calculate the speed of the propelled particles. At the instant of shock unloading and foil deformation, particles gain very high speeds, but soon are decelerated from the very high resistance of the ambient air. A graph of velocities of particles as a function of time and distance is shown in Fig. 5. An abrupt slowdown of the particles is observed in the first few microseconds of their motion, and in later times deceleration is more gradual.

Fig. 6. shows the plastically deformed 100 μm thick aluminum foil due to shock wave unloading. The measured deformation is about 185 μm, and taking into account Eq. (3) we obtain the value of about 65 GPa for the pressure of the shock wave. Considering the order of magnitude, this is in good agreement with Eq. (1), because the energy deposition in the ablation spot was 0.25 GW (a laser pulse of 1.5 J with a 6 ns duration), in a spot with 4 mm diameter. Calculations for the initial and impact particle velocities from Eqs. (4) and (6) result into the values

of 5.8 mm/μs and 0.4 mm/μs, respectively. In these calculations we considered that particles were of spherical shape, with 1-3 μm diameter, and the soft target (gelatin) was 10 mm away from the foil.

Particles delivered ballistically to the gelatin did not cause any apparent damage to the surface other than perforation. They were spread in an area with the diameter of a few millimeters and reached depths up to 1 mm, as shown in Fig. 7a. In the case of rat liver, particles reached depths up to the value of 100 μm, as shown in Fig 7b.

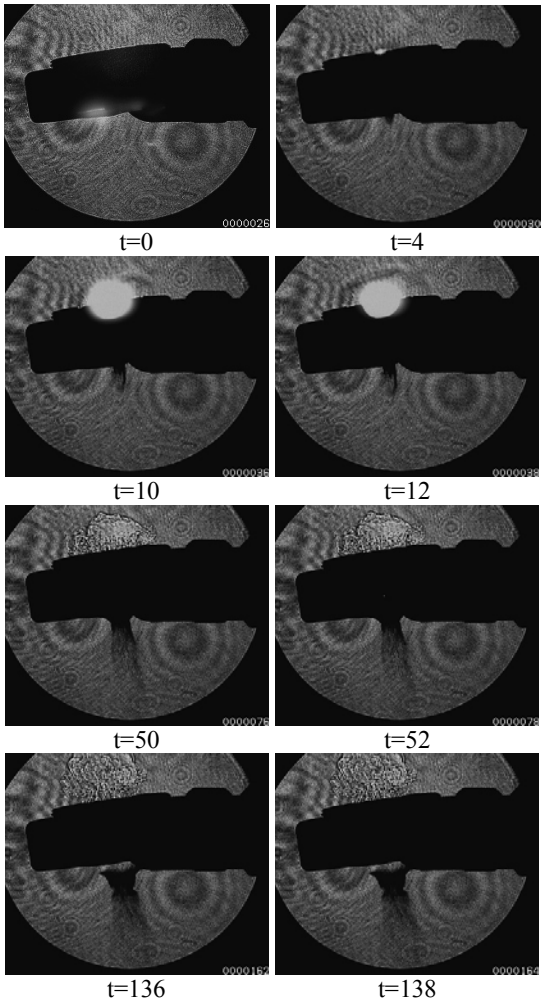

Fig. 4. A series of shadowgraph images showing the propulsion of microparticles by laser ablation. Below each image is designated the time in microseconds after the ablation. The horizontal size of the image frame corresponds to 9 cm.

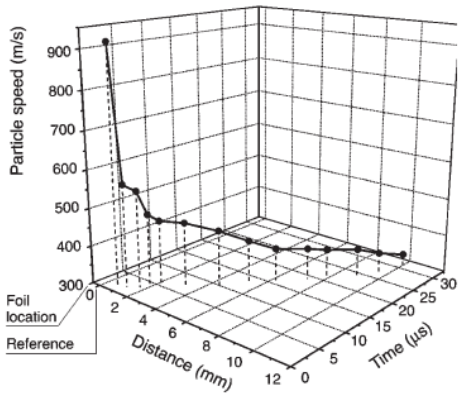

Fig. 5. Particle velocity vs. distance and time from the shadowgraphs. At the initial stage, each data point is taken at one microsecond interframe.

Fig. 6. The plastically deformed aluminum foil due to shock wave unloading.

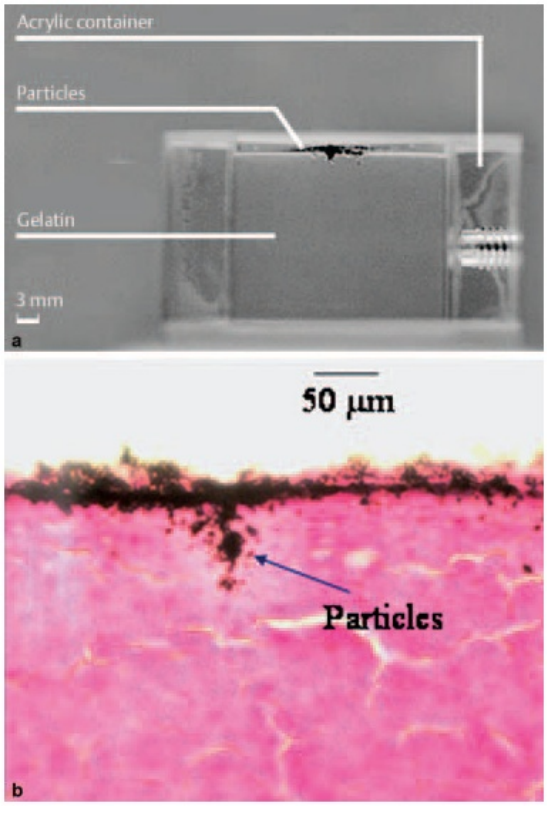

Fig. 7. Tungsten particles delivered by laser ablation into a) 3% gelatin, b) rat liver tissue. (From Ref. 3.)

Conclusions and future prospects

Particle propulsion by means of laser ablation provides an alternative way for drug delivery. The presented study and experiment show that particles can be accelerated up to hypersonic velocities and penetrate hundreds of micrometers into soft tissue.

Future prospects for this research lay can be directed into two paths. One would be further development on the understanding of mechanisms with the aim of reaching higher efficiencies of the laser irradiation - shock wave coupling, with the focus on what material is the best to be used as foil. An important parameter to be investigated by varying for the best efficiency is the surface motion after shock unloading. In this presentation, this parameter was calculated, but there exist experimental techniques, such as VISAR or Mach-Zehnder interferometry, which can directly give experimental values for the velocity of the surface.

The other, perhaps more immediate path of development, is further miniaturization of the delivery system and its coupling with endoscope for delivery to internal organs. One way to address this issue is to transmit the laser light through an optical fiber that can withstand high power pulses. The other aspect of this work that needs attention is research on producing delivery systems with controllable particle velocities and uniform distribution in space, with the ratio between spread diameter and penetration depth as small as possible.

References

1) T. M. Klein, E. D. Wolf, R. Wu, and J. C. Sanford, High-velocity microprojectiles for delivering nucleic acids into living cells, *Nature*, **327**, 1987, pp. 70-73
2) M. A. F. Kendall, The delivery of particulate vaccines and drugs to human skin with a practical, hand-held shock tube-based system, *Shock Waves*, **12**, 2002, pp. 23-30
3) V. Menezes, K. Takayama, T. Ohki, and J. Gopalan, Laser-ablation-assisted microparticle acceleration for drug delivery, *Applied Physics Letters*, **87**, 2005, 163504
4) C. R. Phipps, J. R. Luke, G. G. McDuff, and T. Lippert, Laser ablation powered mini-thruster, High-Power Laser Ablation, Proc SPIE Vol 4760, 2002, pp. 833-842
5) D. von der Linde, and K. Sokolowski-Tinten, The physical mechanisms of short-pulse laser ablation, *Appl. Surf. Sci.*, **154-155**, pp. 1-10
6) L. Berthe, R. Fabbro, P. Perye, and E. Bartnicki, Wavelength dependent of laser shock-wave generation in the water-confinement regime, *J. Appl. Phys.*, **85** (11), 1999, pp. 7552-7555
7) B. H. Ripin, et al., Laser-plasma interaction and ablative acceleration of thin foils at 10^{12}-10^{15} W/cm^2, *Phys Fluids*, **25** (5), 1980, pp. 1012-1030
8) B. P. Fairand, and A. H. Clauer, Laser generation of high-amplitude stress waves in materials, *J. Appl. Phys.*, **50** (3), 1979, pp. 1497-1502
9) J. Dehn, A unified theory of penetration, *Int. J. Impact Eng.*, **5**, 1987, pp. 239-248
10) B. Merchant, Gold, the Noble metal and paradoxes of its toxicology, *Biologicals*, **26**, 1998, pp. 49-59